JOURNAL OF MATERIALS SCIENCE **33** (1998) 5855–5872

Heat treatment effects on SiC fiber

P. R. SMITH, M. L. GAMBONE
Materials Directorate, Wright Laboratory, WL/MLLM, WPAFB, OH 45433

D. S. WILLIAMS
Southwestern Ohio Council for Higher Education (SOCHE), Dayton, OH 45420

D. I. GARNER
University of Dayton Research Institute, Dayton, OH 45469

The Wright Laboratory Materials Directorate at Wright-Patterson AFB has been spearheading the development and evaluation of a new class of metal matrix composites based upon continuous SiC fiber reinforcement of orthorhombic phase containing titanium aluminide matrices. These composites (O TMCs) will be subjected to thermal exposures during primary and secondary component processing, and possibly also during heat treatments to optimize matrix-dominated mechanical performance. Such thermal excursions must not degrade the SiC fiber reinforcement, hence compromising resulting composite properties. Therefore, the effects of heat treatment on the room temperature tensile strength of continuous SiC fibers were studied. The fibers examined included: Trimarc 1®, SCS-6, Ultra SCS and an experimental large diameter version of Ultra SCS. The fibers were heat treated below and above the beta solvus temperature of the orthorhombic matrix alloy utilized for this study, Ti-22Al-23Nb (at %). The fibers were evaluated for ambient temperature tensile strength in the following conditions: (1) as-received: (2) heat treated in vacuum; and (3) consolidated into Ti-22Al-23Nb, heat treated in vacuum, and chemically extracted. Fiber microstructure and fracture analysis was accomplished via secondary scanning electron microscopy (SEM). Chemical reactions between fiber core and the SiC, and between the SiC fiber and the Ti-22Al-23Nb matrix, were also studied by SEM.

1. Introduction

Since 1992, the Materials Directorate has been investigating a class of titanium aluminide matrix composites (i.e. O TMCs) based upon the ordered orthorhombic phase, Ti_2AlNb. These orthorhombic titanium matrices have as their main attributes: improved chemical compatibility with SiC reinforcing fibers, increased room and elevated temperature tensile strength, improved fracture resistance and enhanced elevated temperature creep performance when compared to their alpha-2 based predecessors [1–3]. However, upon fabrication into structural components, it is expected that these O TMCs will undergo multiple thermal exposures during primary and secondary processing. In addition, it is possible that these composite matrices may require heat treatment in order to maximize matrix-dominated mechanical performance. It is imperative that the thermal excursions associated with either heat treatment and/or the component processing cycles do not degrade the load carrying capabilities of the reinforcing SiC fibers. The objective of the subject study is to examine the effect of thermal treatments on the residual room temperature tensile strength of a variety of continuous SiC fibers being considered as potential reinforcements for O TMCs.

2. Experimental

Four continuous SiC fibers were selected for the subject study: Trimarc 1®, SCS-6, Ultra SCS and large diameter Ultra SCS. The first of these fibers, Trimarc 1® is a $\sim$127 μm diameter fiber deposited by chemical vapor deposition (CVD) onto a 12.5 μm tungsten core and was manufactured by Amercom Inc. (Chatsworth, CA). The remaining three fibers were all manufactured by Textron Specialty Materials (Lowell, MA) using CVD processing. The SCS-6 fiber is $\sim$142 μm in diameter and is produced via single-stage CVD deposition onto a 33 μm diameter carbon monfilament (CMF). The Ultra SCS fiber was developed as a higher strength alternative to the SCS-6 fiber. It is roughly the same diameter as the SCS-6 fiber ($\sim$140 μm) and it too is deposited in a single stage CVD process upon a 33 μm CMF. The last fiber, the large diameter Ultra SCS was at the time of this study in the preliminary stages of experimental development. This fiber is on the order of $\sim$184 μm in diameter and has been CVD deposited again in a single stage reactor on a 42 μm CMF. Microstructural details for each fiber are provided later.

The matrix selected for evaluation is the orthorhombic composition, Ti-22Al-23Nb (at %) which the Materials Directorate has been examining as a baseline

representative of this class of titanium aluminides. This alloy was obtained in thin foil (∼125 μm) form from Texas Instruments via conventional ingot reduction practices incorporating as a final step, unidirectional cold rolling. The details of the ingot to foil processing can be found elsewhere [4]. These cold rolled foils were stacked in an alternating fashion with SiC fiber mats and hot isostatically press consolidated into four-ply, unidirectional composites at temperatures well below the beta solvus of the Ti-22Al-23Nb foil, which was determined to be ∼1125 °C. Recent studies [5] on "neat" (i.e. unreinforced consolidated foils) Ti-22Al-23Nb had indicated that this alloy could be heat treated to increased levels of room temperature strength, creep resistance and in some cases improved room temperature ductility. These heat treatments were modified in the present study to account for increases in the beta solvus temperature due to carbon dissolution from the SiC fiber during composite fabrication [6]. The two heat treatments selected include solutionizing just below the beta solvus (subtransus) and just above the beta solvus (supertransus) of the Ti-22Al-23Nb matrix, followed by slow cooling directly to an isothermal aging condition. The subtransus heat treatment had been shown to provide the best balance of "neat" mechanical properties, while the supertransus treatment yielded the best high temperature creep performance. It should be noted that the heat treatments were selected to be compatible with (and possibly incorporated into) the composite/component fabrication cycle. The fibers were encapsulated in tantalum foil to act as an oxygen getter, put in a glass tube, evacuated with a mechanical pump (∼10E-03 torr) which was backfilled with high purity helium (99.9999%) and sealed, and were then heat treated. The specific heat treatments utilized were:

1085 °C/2 h + cool@2.8 °C/m to 815 °C/8 h/FC* (subtransus)

1160 °C/2 h + cool@2.8 °C/m to 815 °C/8 h/FC* (supertransus)

*Furnace cooled ∼25 °C/min

Each type of SiC fiber examined was produced in a single reactor run. In order to assess the effects of fiber/matrix chemical interaction during composite consolidation and subsequent heat treatment, small specimens (12.5 mm × 510 mm) were cut from SiC/Ti-22Al-23Nb panels and were subjected to heat treatment. Fibers from these composite samples were chemically extracted using 10% bromine in methanol saturated with tartaric acid. This solution had previously been shown to be successful in extracting SiC fibers from a titanium matrix without any change in tensile strength distribution [7].

The four types of SiC fibers were tensile tested at room temperature using 25 mm gage section at a constant cross-head speed of 20 mm/min. The tests were conducted on a compact horizontal test machine which was developed by the University of Dayton Research Institute under USAF Contract No. F33615-94-C-5200 at Wright-Patterson Air Force Base, Ohio. Closed-loop computer control was used to acquire data during testing, as well as to control test conditions. Displacement was measured with a commercial scanning laser system by using platinum wire "flags" that were hung 15–20 mm apart in the gage length. The load was measured using a 100 kg load cell, while the fibers were held in place by a compressive force applied through the use of aluminum foil-lined grips. The aluminum foil was used to prevent damage to the fiber surface during testing. This rigid grip system also acted to minimize bending stresses during testing. In order to obtain statistically meaningful results, approximately 50 tests were run per condition for each fiber type. (Note: only ∼25 tests/condition could be run on the large diameter Ultra SCS due to limited fiber availability). Tests were conducted on each fiber type under the five aforementioned conditions (i.e. as-received, 1085 °C Solution HT, 1085 °C Solution HT + Extracted, 1160 °C Solution HT and 1160 °C Solution HT + Extracted). Fiber tensile strength was calculated from the maximum measured load and the cross-sectional area determined from a mean fiber diameter assuming that the fibers were cylindrical. The mean fiber diameter for each fiber type and condition was measured using a non-contact digital micrometer at a magnification of 200×. Only failures which occurred in the gage length were used in the data analysis.

When possible, one or both of the fracture surfaces were preserved and inventoried for examination by scanning electron microscopy (SEM) using secondary electron imaging to assess fracture type and initiation site. However, in some instances the fibers would shatter, particularly for the high strength tests, and in these instances, no information regarding the origin of fracture could be obtained. (Fracture site identification was considerably easier for the weaker Trimarc 1® fiber, than for the higher strength SCS-6, Ultra SCS and large diameter Ultra SCS fibers. As such, correspondingly more fractographic analysis is provided for the Trimarc 1® fiber during the discussion which follows.)

Transverse cross-sections for each of the fibers were mounted, polished, etched and examined by SEM to characterize their microstructural features and assess their thermal stability. Sample preparation for the fibers included: etching in boiling $NaOH : KNO_3$ for 2 minutes, washing in boiling water for 5 minutes, and immersing in ethanol. In addition, the Ti-22Al-23Nb matrix microstructure and fiber/matrix interface were also examined for effects of heat treatment using backscattered electron imaging (BSE) SEM.

3. Results and discussion

3.1. Matrix characterization

Fig. 1 displays the microstructure of the Ti-22Al-23Nb matrix in the as-consolidated and as-consolidated + heat treated conditions. The as-consolidated microstructure (Fig. 1a) consists of three ordered phases [8]: alpha-2 (dark equiaxed); orthorhombic (gray lenticular); and beta/B2 (light). The microstructure is in a metastable state in that the orthorhombic phase is very fine and has not fully precipitated from the B2. The

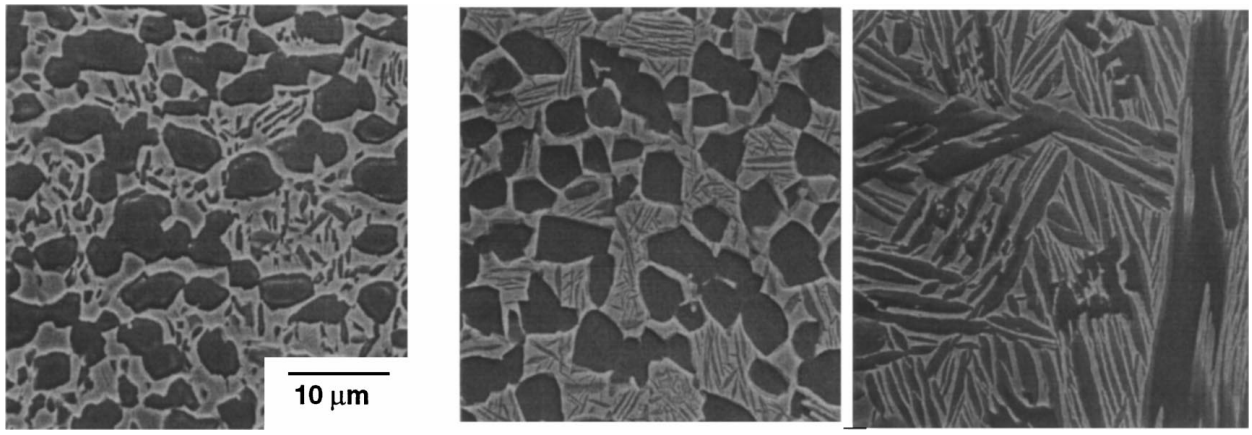

(a) (b) (c)

Figure 1 Ti-22Al-23Nb neat matrix in: (a) as-consolidated, (b) 1085 °C solution HT and (c) 1160 °C solution HT conditions.

relatively high volume fraction of the alpha-2 is due in part to the high levels of oxygen (∼1700 wppm) in the starting foil [9], and possibly due to carbon dissolution from the SiC fiber into the matrix during consolidation. The subtranus heat treatment also results in a three phase microstructure (Fig. 1b). In this case the orthorhombic phase has more fully precipitated from the B2 and has undergone grain growth. As previously noted, this microstructure resulted in the best balance of mechanical properties for neat Ti-22Al-23Nb. The supertransus heat treatment produces a fully transformed two-phase microstructure (Fig. 1c). The large lenticular gray phase is orthorhombic, while the light continuous phase is B2. This microstructure resulted in the best creep resistance for neat matrix studies in Ti-22Al-23Nb.

4. Trimarc 1®

4.1. Fiber structure

This ∼127 μm fiber was produced by CVD processing in a multi-stage "flexible" reactor at Amercom Inc. The salient features of the fiber architecture include a 12.5 μm tungsten core upon which stoichiometric β SiC is deposited. The SiC grows in a columnar fashion and is protected at the surface by the application of a triplex coating system (∼4 μm), which is applied in-line at the end of the CVD process. This coating consists of three alternating layers of "hard" and "soft" carbon with individual layer thicknesses ranging from 0.5 to 2.0 μm. The degree of hardness associated with each of these layers has been suggested to be dictated by the level of and size of the dopent SiC particles. Details concerning the development and production of the Trimarc 1® fiber can be found elsewhere [10].

4.2. Tensile properties, microstructure and fracture analysis

4.2.1. As-received

Fig. 2a shows an SEM image of the β SiC portion of the as-received Trimarc 1® fiber wherein it can be seen that the microstructure grows radially outward in a columnar fashion from the tungsten core. Fry [10] has shown that during fiber production, typically {1 1 1} close-packed planes of the cubic β SiC orient normal to the radial direction. An as-received fracture surface (Fig. 3a) shows that a chemical reaction takes place between the tungsten core and the SiC during fiber manufacturing, forming a layer of tungsten carbide (∼0.38 μm). The outer portion of this reaction layer also contains Kirkendall porosity formed as the result of the diffusion of carbon into and reaction with the tungsten core. Previous studies [11] have indicated this porosity within the tungsten carbide layer acts as a source for crack

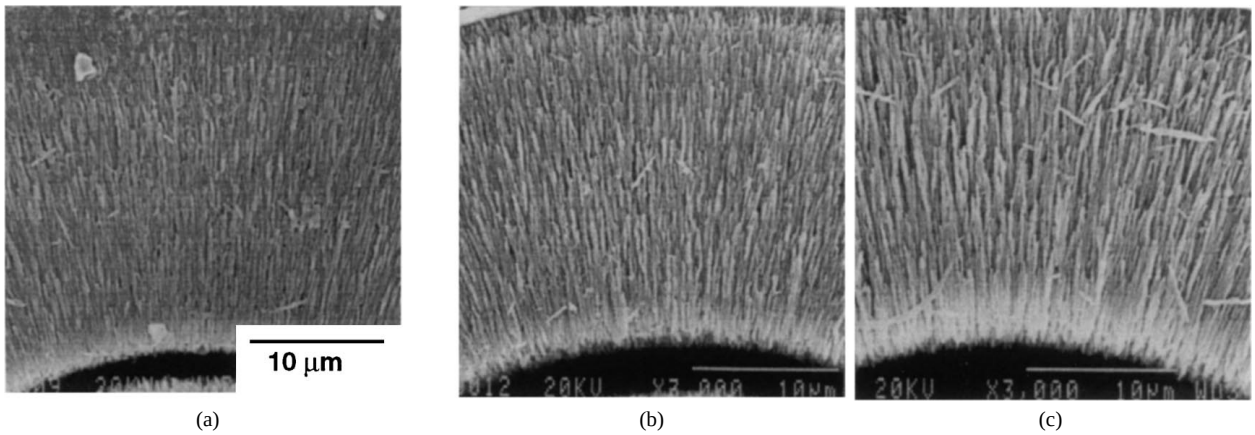

(a) (b) (c)

Figure 2 BSE SEM photos of Trimarc 1® β SiC region in: (a) as-consolidated, (b) 1085 °C solution HT and (c) 1160 °C solution HT conditions.

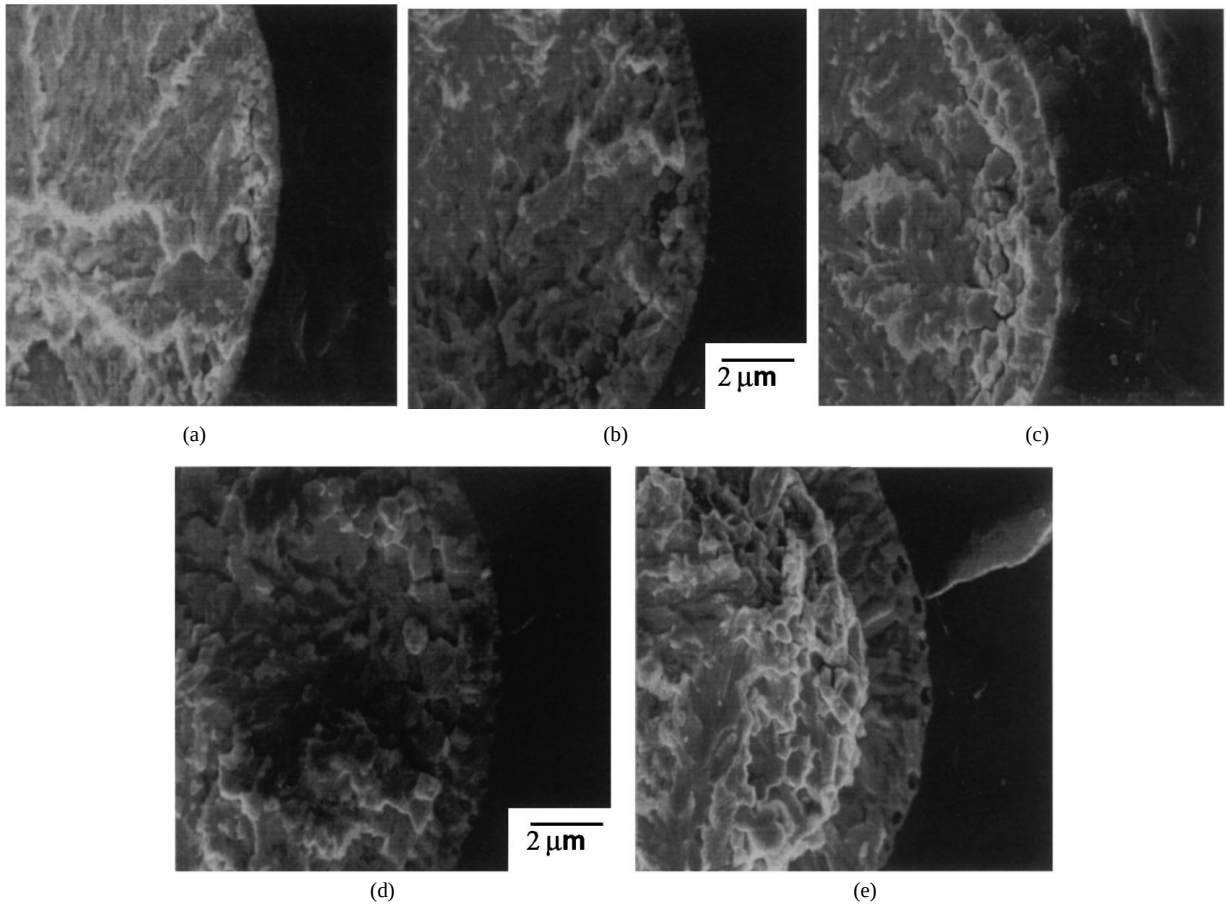

Figure 3 Tungsten core/SiC reaction in Trimarc 1® fiber for: (a) as-received, (b) 1085 °C solution HT, (c) 1085 °C solution HT + extracted, (d) 1160 °C solution HT and (e) 1160 °C solution HT + extracted conditions.

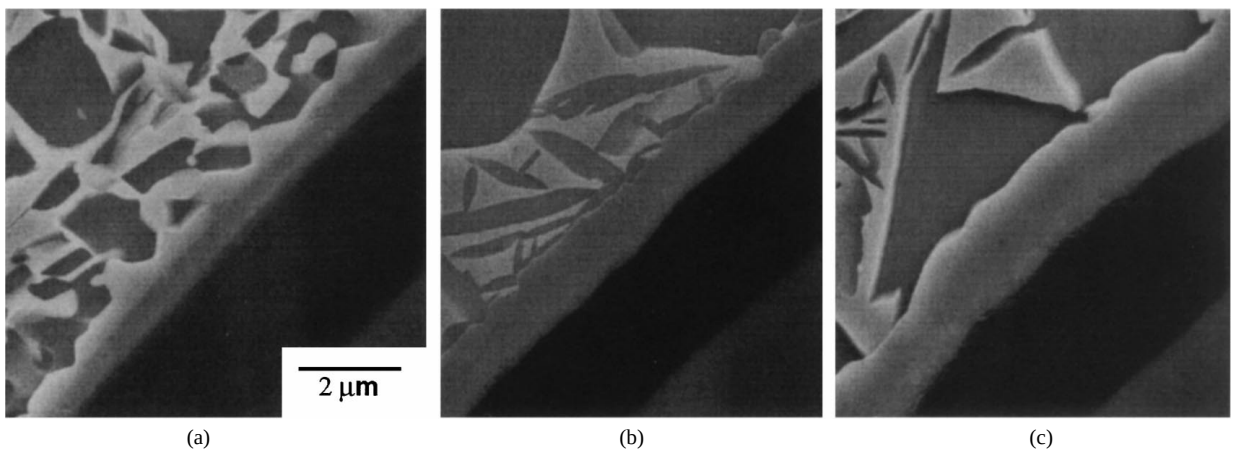

Figure 4 Trimarc 1®/Ti-22Al-23Nb reaction for: (a) as-consolidated, (b) as-consolidated + 1085 °C solution HT and (c) as-consolidated + 1160 °C solution HT conditions.

initiation and fiber strength degradation. In addition to this internal reaction zone, a chemical reaction also takes place at the SiC fiber/matrix interface ($\sim$0.51 μm) as shown in Fig. 4a, upon consolidation of the Trimarc 1® fiber into the Ti-22Al-23Nb matrix. The fiber/matrix reaction products have previously been shown to consist primarily of a complex combination of titanium and aluminum carbides, as well as titanium silicides [12, 13]. These reaction products are extremely brittle in nature and are prone to cracking when loaded either by internally generated residual stresses or by externally applied forces leading to composite mechanical property degradation. It is therefore desirable to limit the size of this reaction layer from the standpoint of composite mechanical performance. The room temperature tensile strength of the as-received fiber is depicted in Fig. 5 as a function of probability of survival at a given stress level. It can be seen that the distribution is very tight with 98% of failures at strengths between 2800 and 3200 MPa. The mean strength for the as-received condition is on the order of 3080 MPa with most failures initiating in or near the tungsten core region of the fiber (Fig. 6a). Indeed, >86% of the failures which could be identified initiated in or near the fiber core. There were

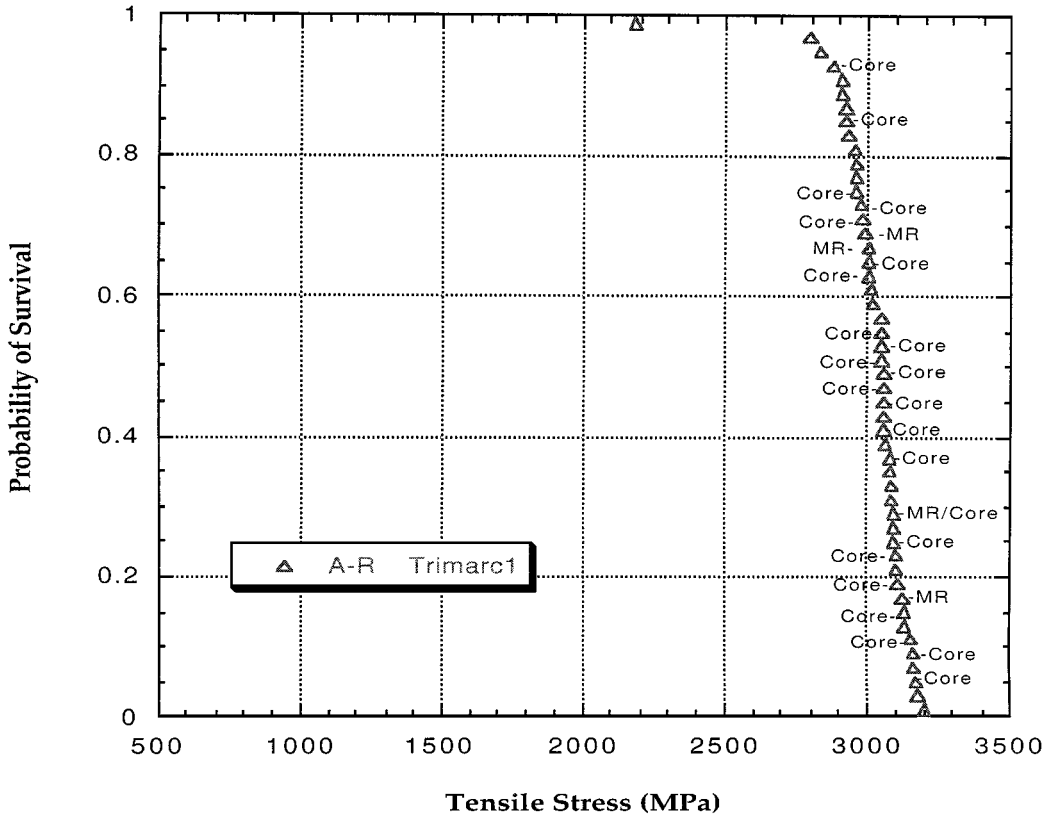

Figure 5 As-received Trimarc 1® strength.

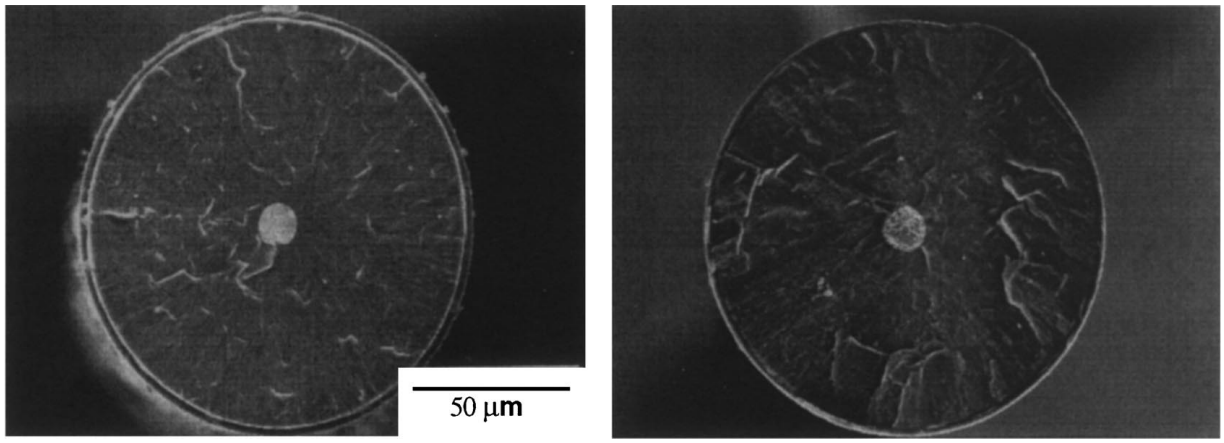

(a) (b)

Figure 6 Secondary SEM images of Trimarc 1® fracture surface for as-received condition illustrating (a) core initiation and (b) mid-radius initiation.

a few failures (13.5%) identified near the mid-radius of the fiber (Fig. 6b), however, the failure strengths associated with this location (3053 MPa) were very similar to those attributed to core failure (3050 MPa).

4.2.2. Subtransus heat treated

The tensile strength for the 1085 °C solution HT condition for Trimarc 1® fiber is shown in Fig. 7. The mean strength has dropped relative to the as-received condition (to 2766 MPa), with the percentage of core failures actually increasing to >96%. The width of the β SiC columnar grain structure has increased slightly (Fig. 2b), suggesting that the structure of the fiber may not be totally stable at this heat treatment temperature (i.e. 1085 °C). Fig. 3b shows that the reaction between the tungsten core and SiC has essentially doubled ($\sim$0.74 μm) compared to the as-received condition. There was only one failure identified with the surface of the fiber and its strength value (2707 MPa) was very similar to that observed for core initiations (2741 MPa). Since the primary failure site appears to be at or near the tungsten core, it can be concluded that increased reaction at the core/SiC interface is the controlling factor in the observed strength reduction.

4.2.3. Subtransus heat treated + extracted

The Trimarc 1® fiber tensile strength in the 1085 °C Solution HT + extracted condition is shown in Fig. 8. In this case the fiber was consolidated into a Ti-22Al-23Nb matrix, heat treated and chemically extracted for

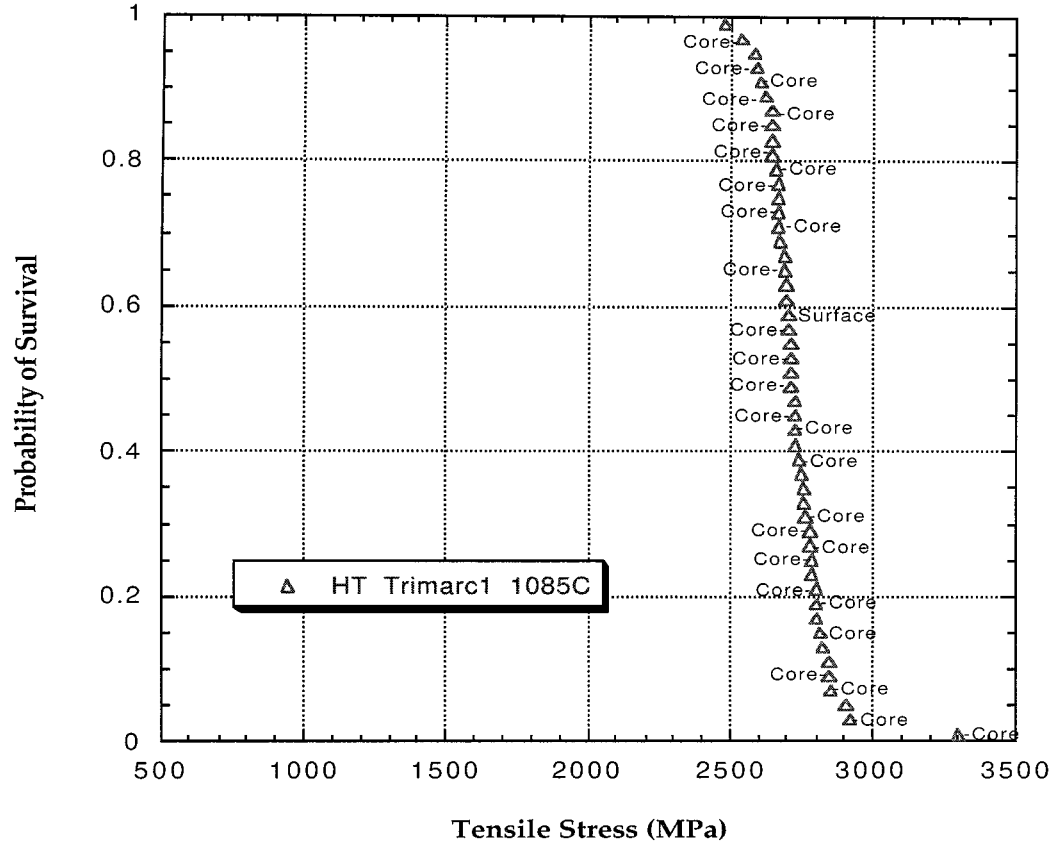

Figure 7 Trimarc 1® fiber strength after 1085 °C solution HT.

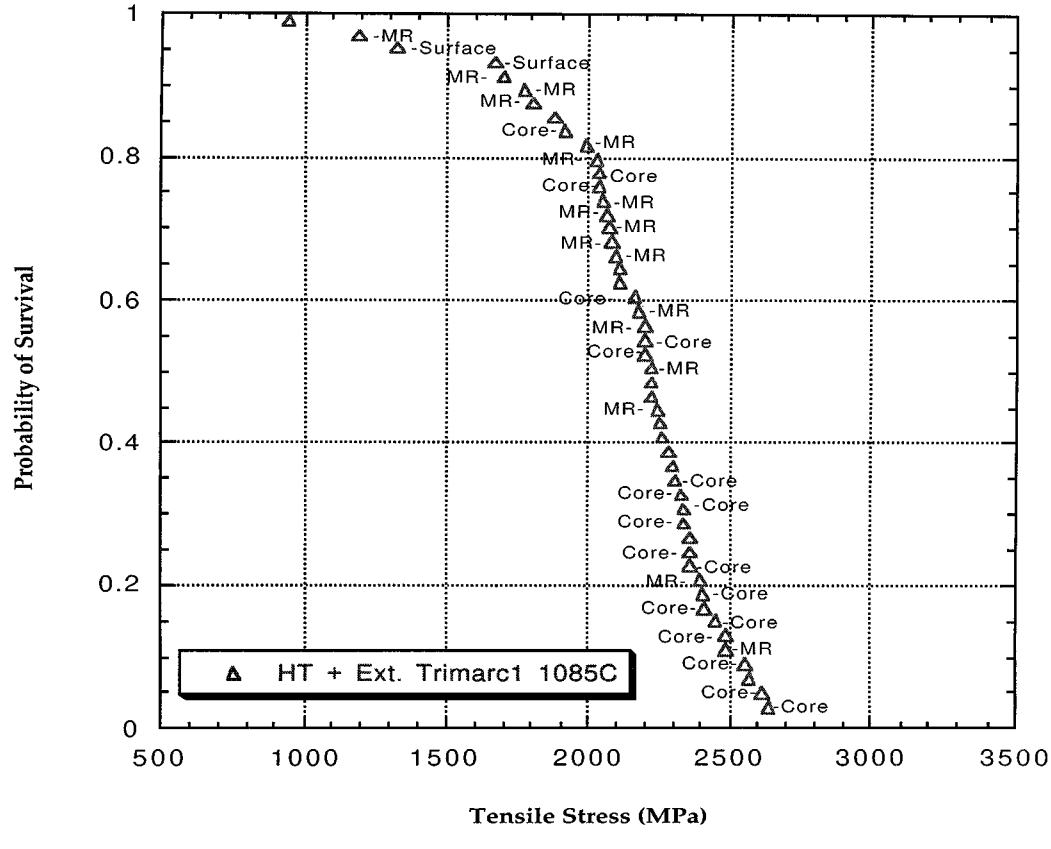

Figure 8 Trimarc 1® fiber strength in 1085 °C solution HT + extracted condition.

testing. The mean fiber strength has dropped to 2272 MPa. Furthermore, the fiber appears to fail both at regions near and around the core (47%), and also near the mid-radius of the fiber (46%). The average strength values associated with the mid-radius failures (2006 MPa) was noticeably less than for core failures (2334 MPa). The core/SiC reaction zone has increased to 1.05 μm (Fig. 3c) when compared to the subtransus heat treated

condition (0.74 μm) due to the additional thermal exposure required for composite fabrication. Furthermore, the reaction zone at the fiber/matrix interface (Fig. 4b) has increased by a factor of 3× (to 1.15 μm) when compared to the as-fabricated condition. There were two failures identified at the surface of the fiber whose strength values were very low (1476 MPa). However, the most prominent failure site for low strength failures appears to be near or at the mid-radius of the SiC fiber. The propensity for increased number of low strength failures at the mid-radius may be related to manufacturing defects in the fiber in combination with residual stresses arising during composite fabrication. The CTE of the matrix is roughly 3× that of the fiber at room temperature. As such, during cool-down from the composite consolidation temperature the fiber is subjected to a large radial compressive residual stress. It is hypothesized that this stress tends to exacerbate the effect of defects near the mid-radius location of the SiC fiber.

4.2.4. Supertransus heat treatment

The fiber strength data for Trimarc 1® subjected to a supertransus heat treatment in vacuum is shown in Fig. 9. The mean fiber strength continues to be degraded (to 2175 MPa). Almost all identifiable failures (>97%) occurred at or near the tungsten core with strength levels (2098 MPa) correspondingly close to the mean strength. In addition, there was very little scatter in the data set with 97% of the failures occurring within a 475 MPa band (1850–2325 MPa). The β SiC grains experience additional growth (Fig. 2c) continuing to suggest that the SiC microstructure is not stable at 1160 °C, however there were no failures identified at the mid-radius region of the SiC layer. The core/SiC reaction zone has increased to 1.21 μm (Fig. 3d), and is likely the controlling mechanism for the additional strength degradation which is observed. There was only a single failure identified with the surface of the Trimarc 1® fiber, however, like most failures of this type, it occurred at a relatively low strength level (1939 MPa).

4.2.5. Supertransus heat treated + extracted

The Trimarc 1® fiber tensile strength for the 1160 °C solution HT + extracted condition is shown in Fig. 10. The mean fiber strength has dropped to 1639 MPa, which represents a 45% decrease when compared to the as-received strength condition. Furthermore, it is noticed that the fiber appears to fail primarily at regions near and around the core (81%). In addition, there were a few low strength failures (10%) in locations found near the mid-radius of the SiC layer of the fiber, and also at the surface the fiber surface (9%). The highest strength failures are associated with the core/SiC reaction zone (1782 MPa). This reaction zone has increased in size to 1.92 μm (Fig. 3e) when compared to the supertransus condition (1.21 μm) due to the additional thermal exposure required for composite consolidation. The failures associated with the mid-radius (1410 MPa) suggest once again that compressive residual stresses arising from CTE mismatch due to composite fabrication may play a role as they had for the subtransus

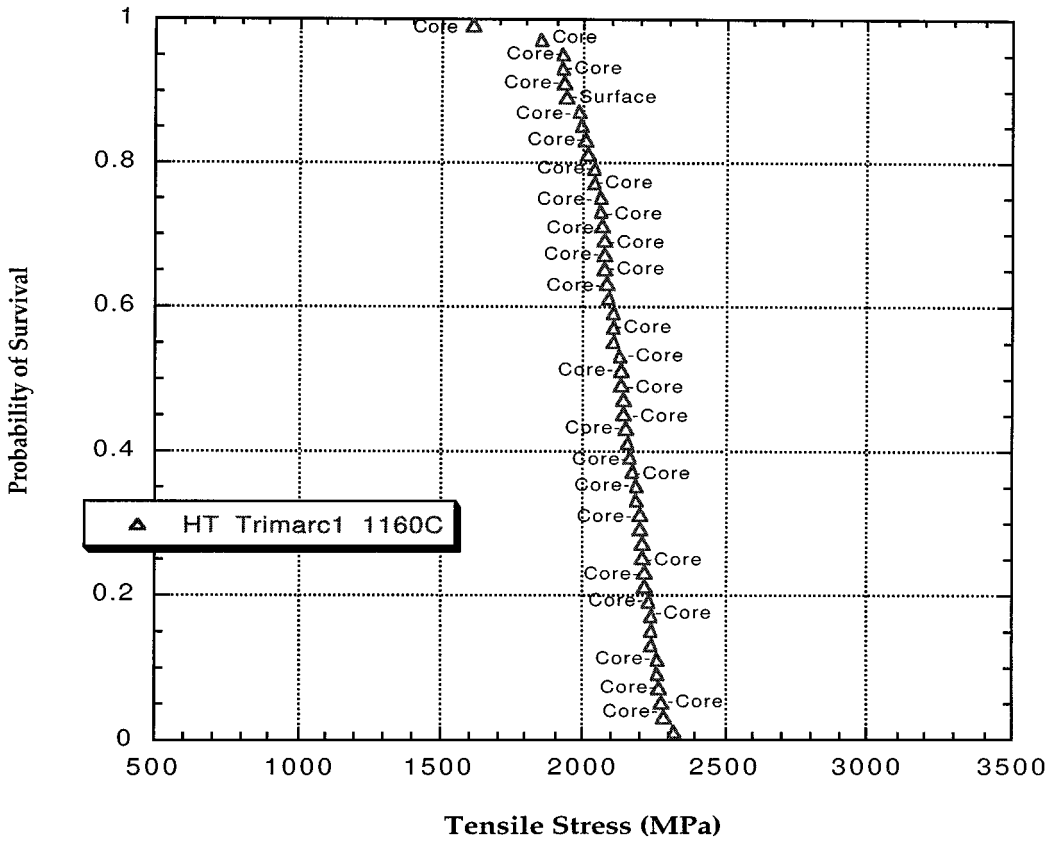

Figure 9 Trimarc 1® fiber strength in 1160 °C solution HT condition.

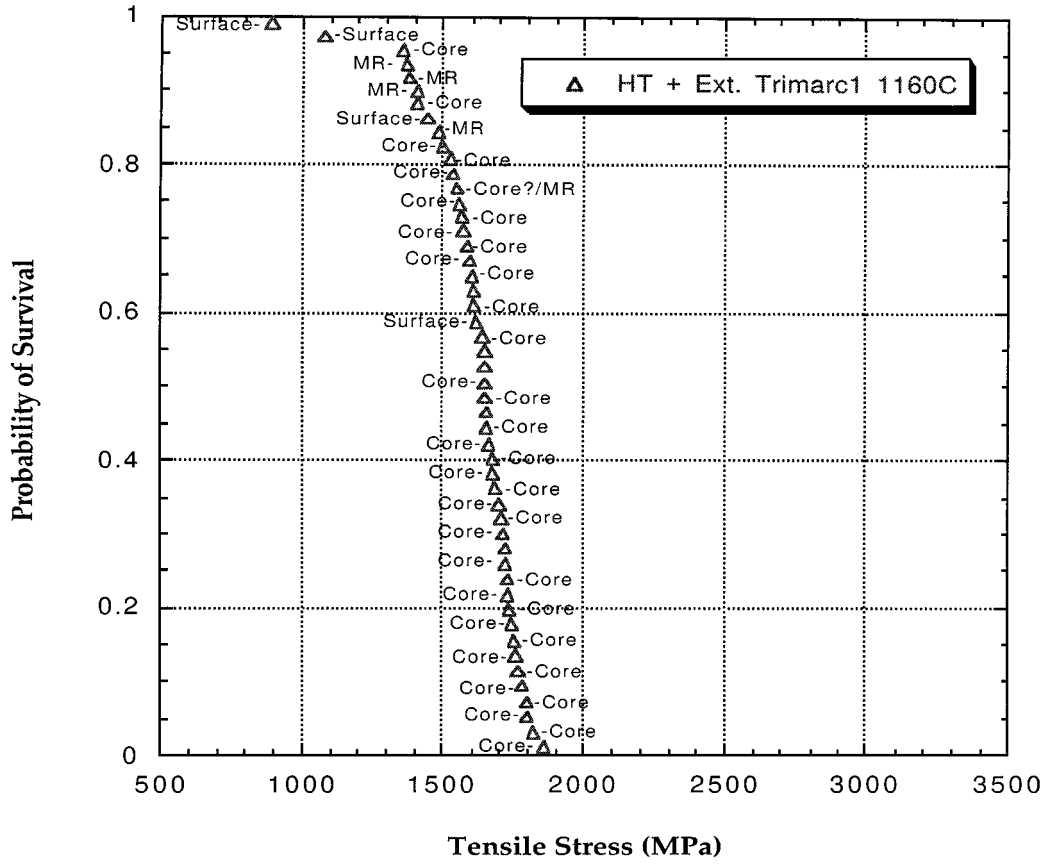

Figure 10 Trimarc 1® fiber strength in 1160 °C solution HT + extracted condition.

heat treated and extracted condition. Furthermore, the lowest strength failures (1255 MPa) occurred at the fiber surface, and may be associated with growth of the fiber/matrix reaction zone (Fig. 4c), which has increased by a factor of 4× (to 1.98 μm) when compared to the as-fabricated condition.

4.2.6. Summary Trimarc 1®

Fig. 11 displays a summary of the effect of heat treatment on the tensile strength of the Trimarc 1® fiber for all conditions, while Table I contains a summary of the fracture analysis data. All heat treatments are seen to degrade the fiber strength below as-received values (up to 45% for the 1160 °C solution HT + extracted condition). In each case a significant number of core initiations are observed with the average strength value for those initiations decreasing with increased thermal exposure. This strength degradation is attributable to the increased reaction between the tungsten core and the SiC during composite consolidation and/or heat treatment. With respect to tungsten core/SiC reaction effects on fiber tensile strength, the Griffith criterion for cracks in brittle materials is thought to apply [i.e. $\sigma = C/\sqrt{x}$; wherein σ = fiber strength (GPa), x = crack length (reaction zone thickness (μm) and C is a constant determined for the as-processed condition]. Table II contains core/SiC reaction zone data along with experimentally determined and calculated values of σ (for core failures) using the Griffith criterion. Although this criterion does predict a strength debit, it would appear it consistently over-estimates the magnitude of the debit by 15–20%.

Similarly, Gambone and Gundel [14] performed a kinetic analysis for Trimarc 1® fiber wherein they were able to determine regions of time at temperature wherein degradation of the fiber tensile strength is

TABLE I Fracture summary for Trimarc 1®

	As-received	1085 °C	1085 °C + Ext	1160 °C	1160 °C + Ext
No. of fractures identified	26/50	30/50	38/52	35/50	45/50
Mean strength (MPa)	3079	2766	2272	2175	1639
% Core mean	86.5	96.6	47.4	97.1	81.1
strength (MPa)	3059	2741	2334	2098	1782
% Mid radius mean	13.5	0	46.1	0	10
strength (MPa)	3053	—	2006	—	1410
% Surface mean	0	3.4	6.5	2.9	8.9
strength (MPa)	—	2707	1476	1937	1255

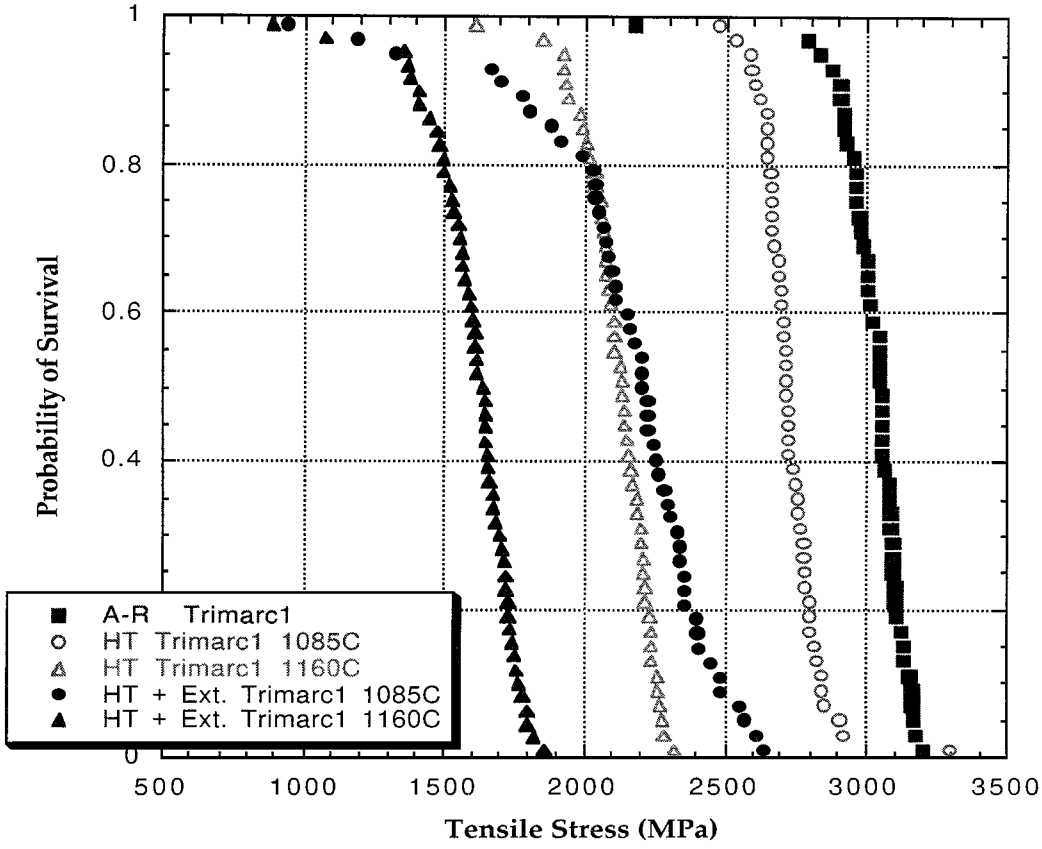

Figure 11 Summary of effect of heat treatment on Trimarc 1® strength.

TABLE II Effect of core/SiC reaction on Trimarc 1® fiber strength

Condition	Reaction zone (μm)	St. dev (μm)	σ, core (GPa)	
			Experimental	Calculated
As-Fabricated	0.38	0.03	3.059	3.080
1085 °C	0.74	0.03	2.766	2.192
1085 °C + Ext'd	1.05	0.06	2.272	1.840
1160 °C	1.21	0.07	2.175	1.714
1160 °C + Ext'd	1.92	0.11	1.639	1.361

expected to occur. The solution heat treatment conditions used in the current study fall in a region very near to where strength degradation would be expected.

In addition, high compressive radial residual stresses due to CTE mismatch between the fiber and matrix act to catalyze mid-radius failures for the heat treated + extracted conditions. There also appears to be a thermal instability of the β SiC microstructure which might be an issue to consider for future development of this fiber. Finally, the increased fiber/matrix reaction associated with the heat treatments within the Ti-22Al-23Nb, may be responsible for the few very low strength failures occurring at the surface of the fiber for the heat treated + extracted conditions.

In conclusion, the degradation observed for the Trimarc 1® fiber suggests this fiber as currently produced is unsuitable for use as a reinforcement in an orthorhombic titanium aluminide matrix for metal matrix composite applications wherein processing and/or heat treatment temperatures are comparable to, or exceed those examined in the subject study.

5. SCS-6

5.1. Fiber structure

A schematic of the SCS-6 fiber is displayed in Fig. 12. Microstructural and chemistry details for this fiber have been described elsewhere [15–18] and are summarized here. This 142 μm diameter fiber is produced by CVD processing in a single-stage reactor. The salient features of the fiber architecture are that the core consists of a 33 μm diameter carbon monofilament (CMF) originally spun from a pitch-based material, which is then sealed by a 1.5 μm thick overcoat of pyrolytic carbon. The β SiC grows in columnar fashion outward from the CMF core forming two distinct zones. The zones consists of subgrains of β SiC with close-packed {1 1 1} planes oriented radially. These subgrains have a large aspect ratio with their length in the radial direction. The first zone which extends approximately 15 μm is relatively fine grained (10–60 nm) and from a compositional standpoint, is slightly carbon rich [19]. Although not depicted in Fig. 12, Ning [15] has determined that the inner zone actually consists of three subzones with thicknesses starting at the pyrolytic coating of 6 μm, 4.5 μm and 4.5 μm, respectively. The second zone is approximately 35 μm wide and exhibits a coarser grain structure (70–140 nm) and is essentially stoichiometric in composition. The change in grain size is attributed to this change in chemistry. The interface between the two growth layers forms what is referred to as the mid-radius of the SiC. Unlike the tungsten core for the Trimarc 1® fiber, the CMF and the SiC are in chemical equilibrium, and as such, there is no observable reaction between the two. The external surface of

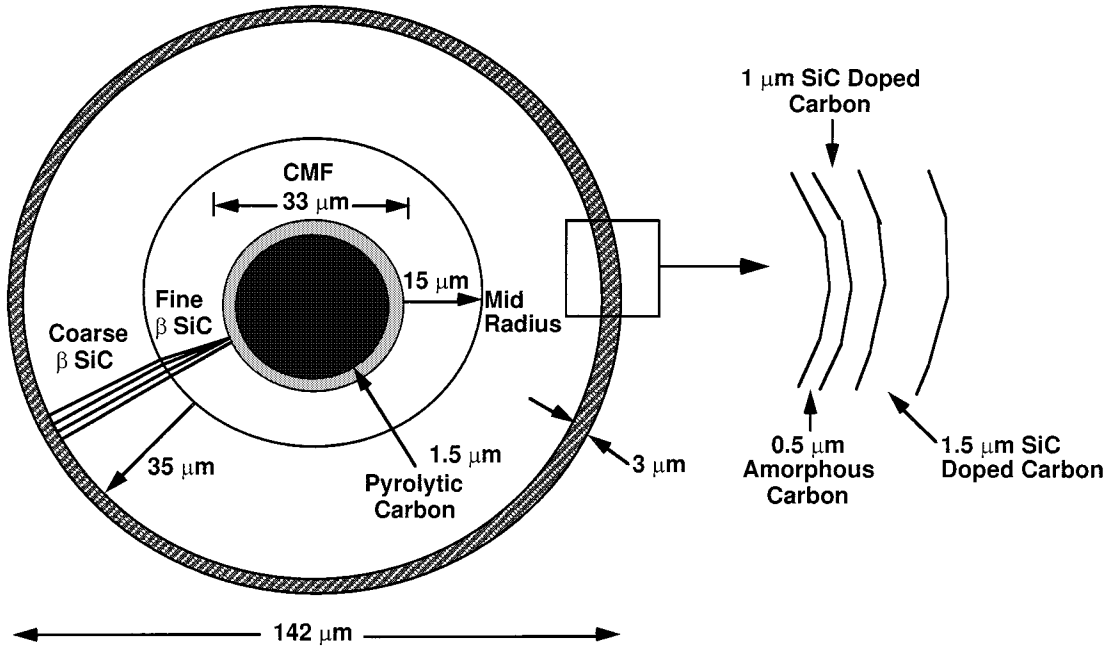

Figure 12 Schematic of SCS-6 fiber.

the fiber is coated with three carbonaceous layers totaling $\sim 3\,\mu$m in thickness, which is used to protect the fiber during handling and to reduce its susceptibility to strength degradation due to chemical reaction within titanium matrices. The first coating layer is amorphous carbon which is approximately 0.5 μm thick and which acts to "seal" the ends of the columnar β SiC. The fiber is then coated with two carbon layers (i.e. double pass) which are doped with β SiC crystallites. The thicknesses of the inner and outer C-rich layers are $\sim 1.0\,\mu$m and 1.5 μm, respectively. The SCS-6 fiber has essentially been adopted as the industry standard for reinforcement of titanium over the last 15 + years, particularly for those instances wherein elevated temperatures (application or processing) preclude the use of tungsten core fibers due to SiC/core reactions.

5.2. Tensile properties, microstructure and fracture analysis

Fig. 13 contains a summary of the heat treatment effect on the tensile strength of SCS-6. The mean strength for the as-received fiber is 4403 MPa, which represents a >40% increase when compared to the as-received Trimarc 1®. Previous results [20] for SCS-6 fiber had indicated isothermal exposures in an inert environment at 1000 °C for up to 700 hours resulted in no strength loss, and no signs of thermal instability in either the fiber coating or β SiC. In the present study, there also appears to be little or no discernible effect of any of the heat treatment conditions on the strength retention of the SCS-6 fiber, including those within the Ti-22Al-23Nb matrix. In fact, 93% of all failures occurred at strength levels in excess of 3000 MPa. Unlike the Trimarc 1® fiber, identification of the primary initiation site via fracture analysis was difficult, in that most of the higher strength fractures tended to be secondary in nature. However, for those fracture surfaces that were retained, the following observations could be made. The highest strength failures were located internally near the core of the fiber (Fig. 14a). There were total of 18 failures which occurred at strength values $\leq$3000 MPa. Of these, 16 initiation sites were identified, and 15 of those occurred at the surface of the fiber (Fig. 14b). (Note: the remaining low strength failure appeared to be associated with a mid-radius initiation.) The fact that the low strength fibers had initiations near the fiber surface might seem to suggest that chemical reaction at the fiber/matrix interface played a role in the strength degradation. Fig. 15 shows the SCS-6/matrix reactions for the as-consolidated, consolidated +1085 °C solution HT, and consolidated +1160 °C solution HT conditions. Although the reaction zone increases as the thermal conditions become more extreme, the protective carbon coating system remains essentially intact (i.e. $>2.0\,\mu$m of coating remains). In fact, half of the surface failures occurred for conditions wherein the fiber was not exposed to the matrix at all (i.e. as-received, 1085 °C solution HT and 1160 °C solution HT conditions). It appears then, that the low strengths associated with the surface failures are a result of manufacturing defects, as opposed to chemical reaction with the matrix. Fry [10] has identified several classes of manufacturing surface defects which tend to reduce SiC fiber strength: CVD growth cones, surface nodules, SiC grains protruding from the fiber surface, surface damage from electrode arcing, and abrasive surface damage during handling. One or more of these defects may have contributed to the low strength values found for the surface failures.

With respect to SiC microstructural stability, Fig. 16 shows the structure of the β SiC as a function of thermal exposure for the SCS-6 fiber. There appears to be only a very slight grain growth even after the supertransus heat treatment.

In conclusion, the SCS-6 fiber retains essentially all of its as-received strength under the heat treatment conditions evaluated, and as such, is suitable for use as a reinforcement in an orthorhombic titanium aluminide

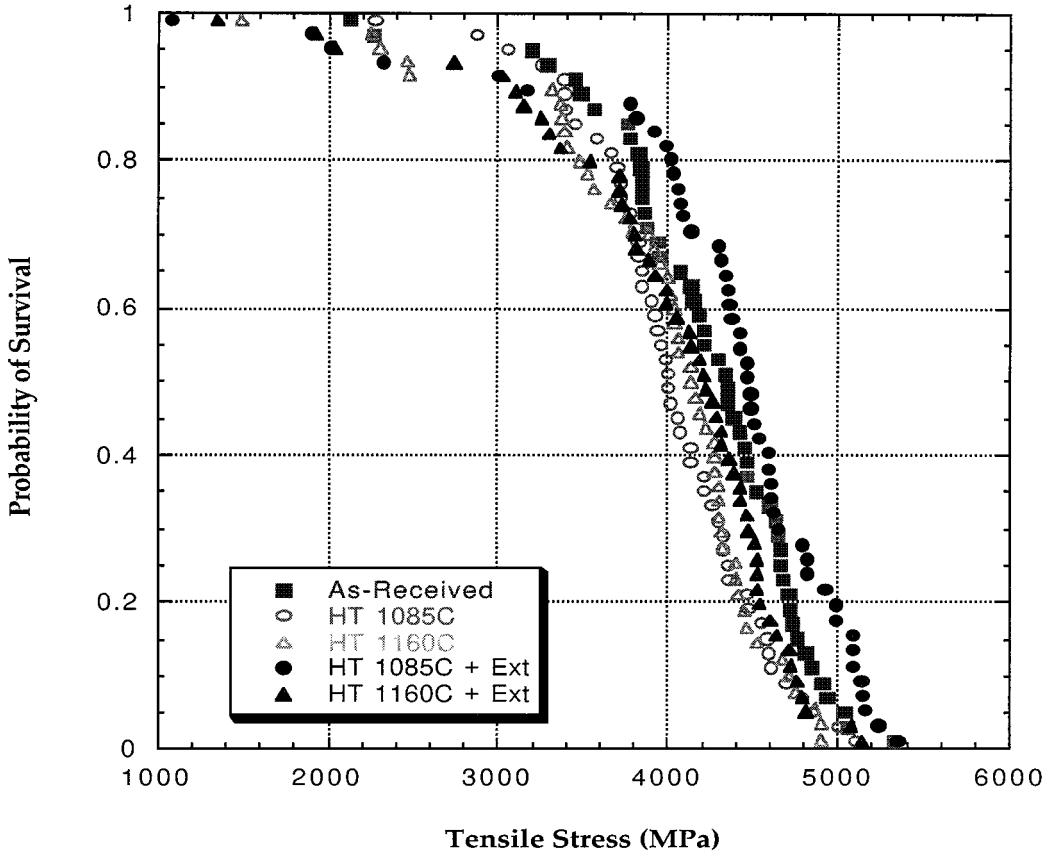

Figure 13 Summary of effect of heat treatment on SCS-6 fiber strength.

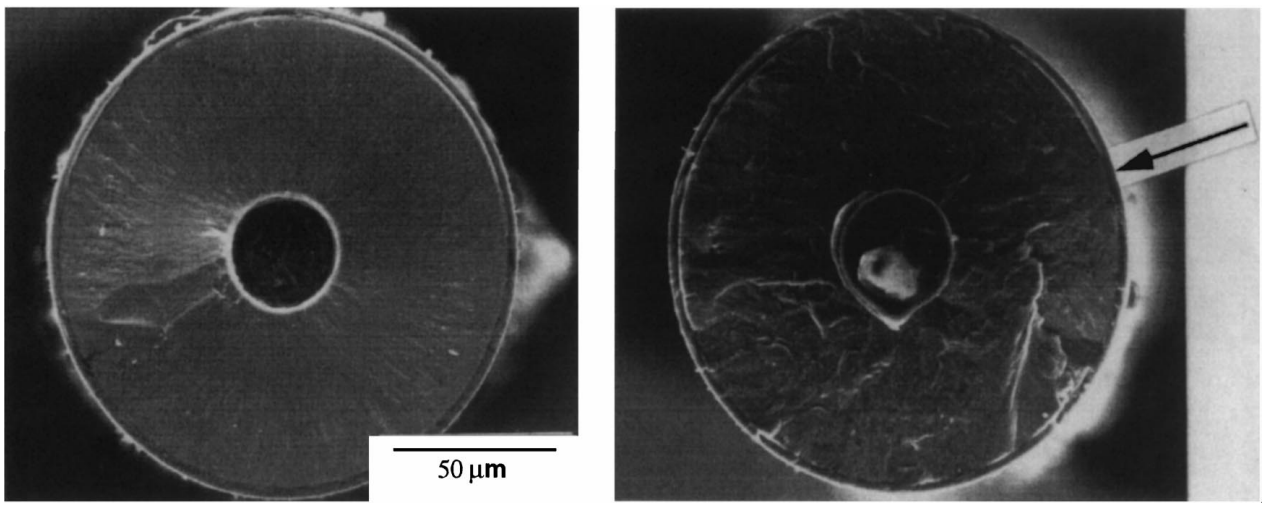

(a) (b)

Figure 14 Fracture surface of SCS-6 fiber illustrating: (a) core and (b) surface initiations.

matrix for metal matrix composite applications wherein processing and/or heat treatment temperatures are comparable to those used in the subject study.

6. Ultra SCS

6.1. Fiber structure

A schematic of the Ultra SCS fiber is displayed in Fig. 17. This 140 μm fiber was developed to replace SCS-6 for those applications requiring increased fiber strength. Unlike the Trimarc 1® which is produced in a multi-stage reactor, the Ultra SCS fiber is produced via single stage CVD processing. The architecture of the Ultra SCS fiber is in some ways similar to that of the SCS-6 fiber. Like the SCS-6 fiber, the deposition of Ultra SCS takes place upon a 33 μm CMF, which again is over-coated with a 1.5 μm thick pyrolytic carbon layer. However, aside from the diameter of the fiber, this is where the similarities end. The microstructure of the SiC portion of the fiber is significantly different in that the grain size is relatively equiaxed and extremely fine in scale (Fig. 18). Furthermore, since the fiber is produced in a single stage reactor, the growth process is continuous with this fine grain structure observed transcending the entire fiber diameter, (i.e. from the

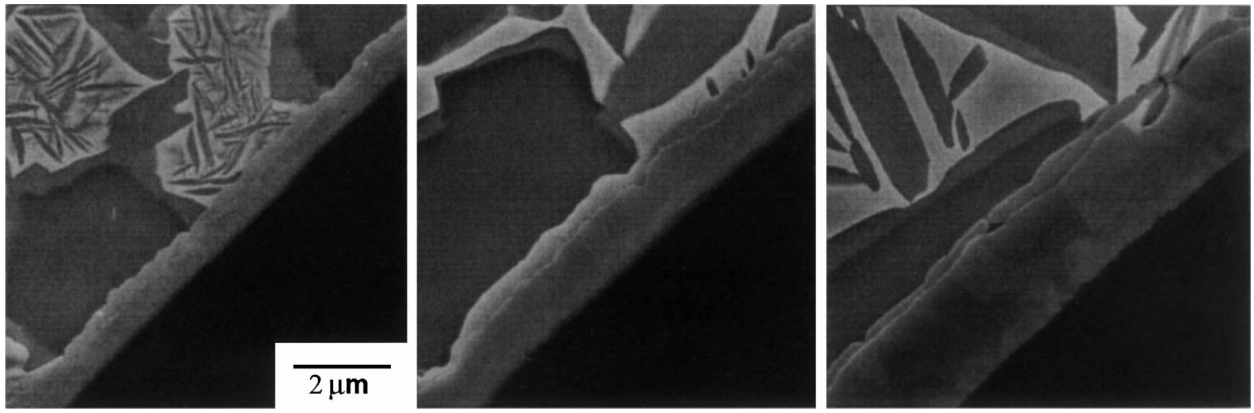

Figure 15 SCS-6/Ti-22Al-23Nb interface reactions for: (a) as-consolidated, (b) consolidated + 1085 °C solution HT and (c) consolidated + 1160 °C solution HT conditions.

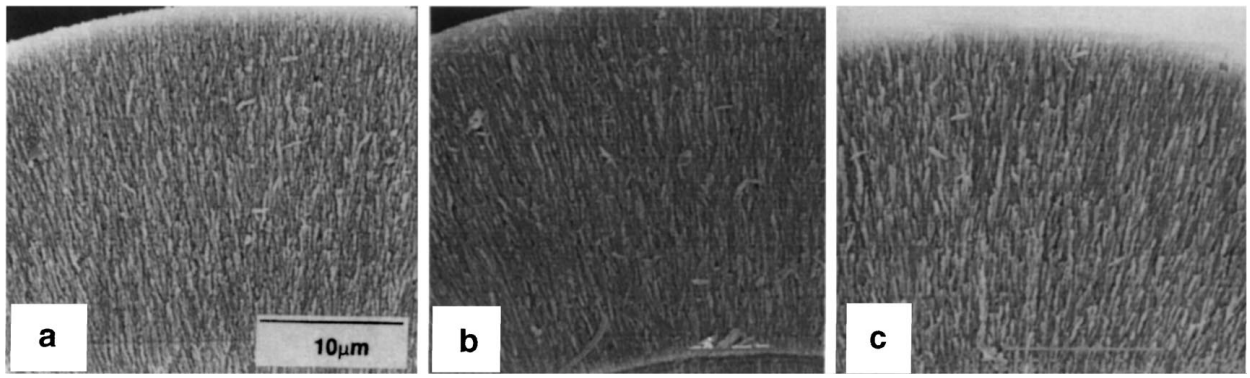

Figure 16 Secondary SEM imaging of β SiC portion of SCS-6 for: (a) as-received, (b) 1085 °C subtranus HT and (c) 1160 °C supertransus HT.

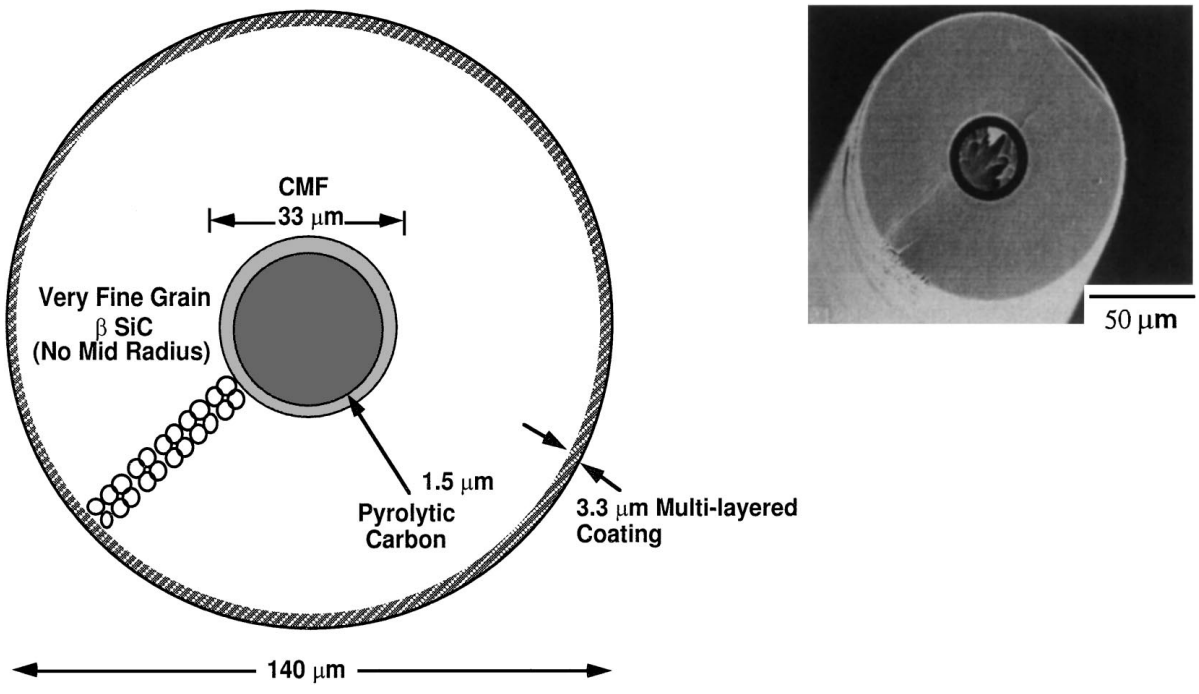

Figure 17 Schematic and secondary SEM image of Ultra SCS fiber.

pyrolytic carbon coating on the core to the external surface coating). As such, there is no mid-radius grain size increase as was observed for the SCS-6 fiber. The surface of the fiber is protected for handlability and chemical reaction with the matrix by a $\sim$3.3 μm thick multi-layered coating. Not only is this coating layer thicker than for SCS-6, but there may also be some chemistry and structural differences as well. However, these and other details were not available from Textron at the time of this writing.

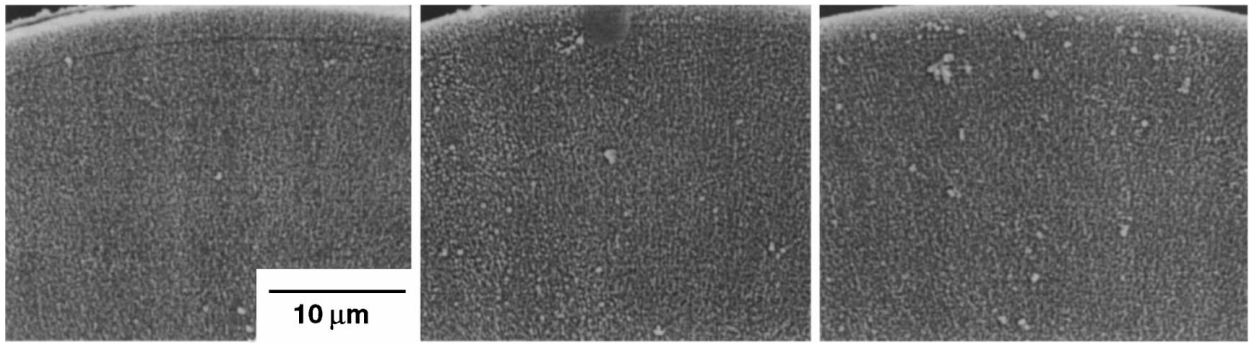

Figure 18 Secondary SEM image of β SiC portion of Ultra SCS fiber in: (a) as-received, (b) 1085 °C solution HT and (c) 1160 °C solution HT conditions.

6.2. Tensile properties, microstructure and fracture analysis

Fig. 19 contains a summary of the heat treatment effect on the tensile strength of Ultra SCS for all conditions. The mean strength for the as-received condition is 5610 MPa, which represents a >25% increase over SCS-6, and >80% over the Trimarc 1® fiber. The source of this high strength is thought to be the fine grained microstructure, and perhaps a modification to the surface coating system. There appears there might be a very modest effect of heat treatment on strength retention, however, 80% of the failures occurred at strengths in excess of 4800 MPa, and 96% in excess of 4000 MPa.

Much like the SCS-6 fiber, the high strength associated with this fiber and the corresponding high energy of fracture make it very difficult to retain and identify fracture surfaces and primary initiation. Most of the failures were secondary in nature (Fig. 20a), however, of the 10 failures occurring at strength levels <4000 MPa, 8 were identifiable, and all originated at the surface of the fiber (Fig. 20b). As for the SCS-6, these surface failures do not appear to be related to chemical reaction with the matrix, as 5 of the 8 were for conditions for which the fiber was not in contact with the matrix. With regard to fiber/matrix chemical reaction, the effect of thermal exposure of reaction zone growth is depicted in Fig. 21. Here it can be seen that the reaction zone is somewhat less uniform and grows at a slightly more rapid rate than for the SCS-6 fiber, lending credence to the possibility that the chemical make-up

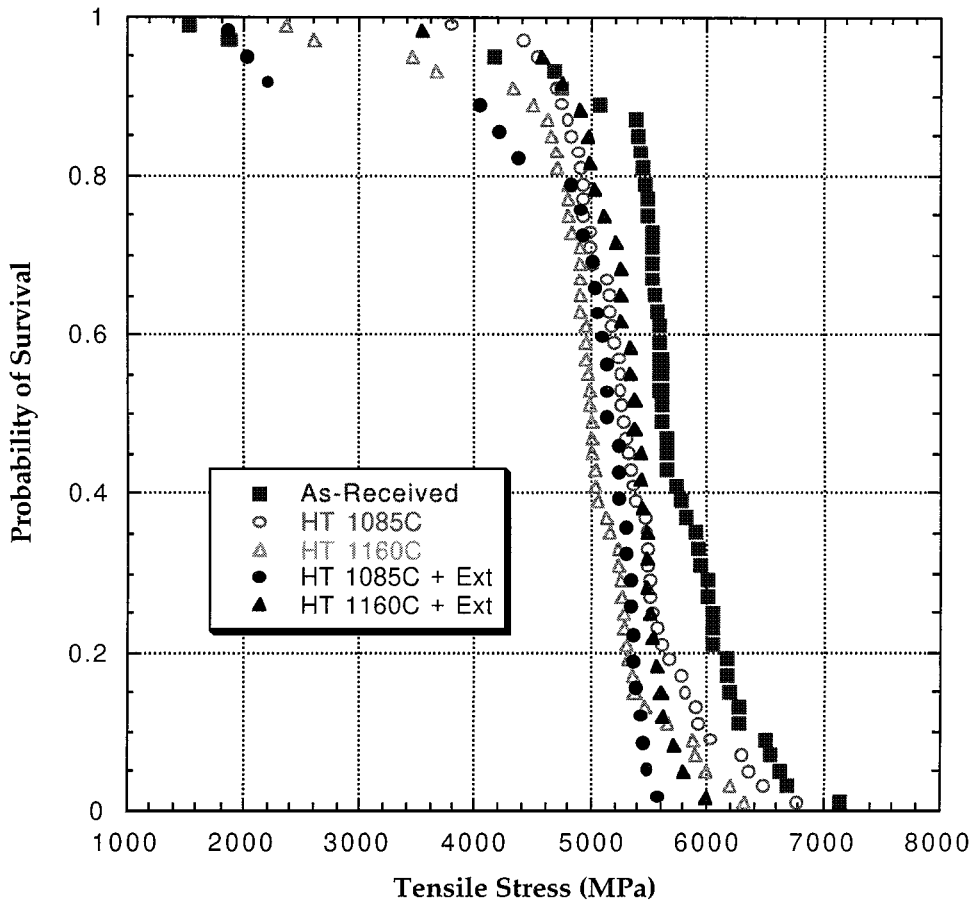

Figure 19 Summary of effect of heat treatment on Ultra SCS strength.

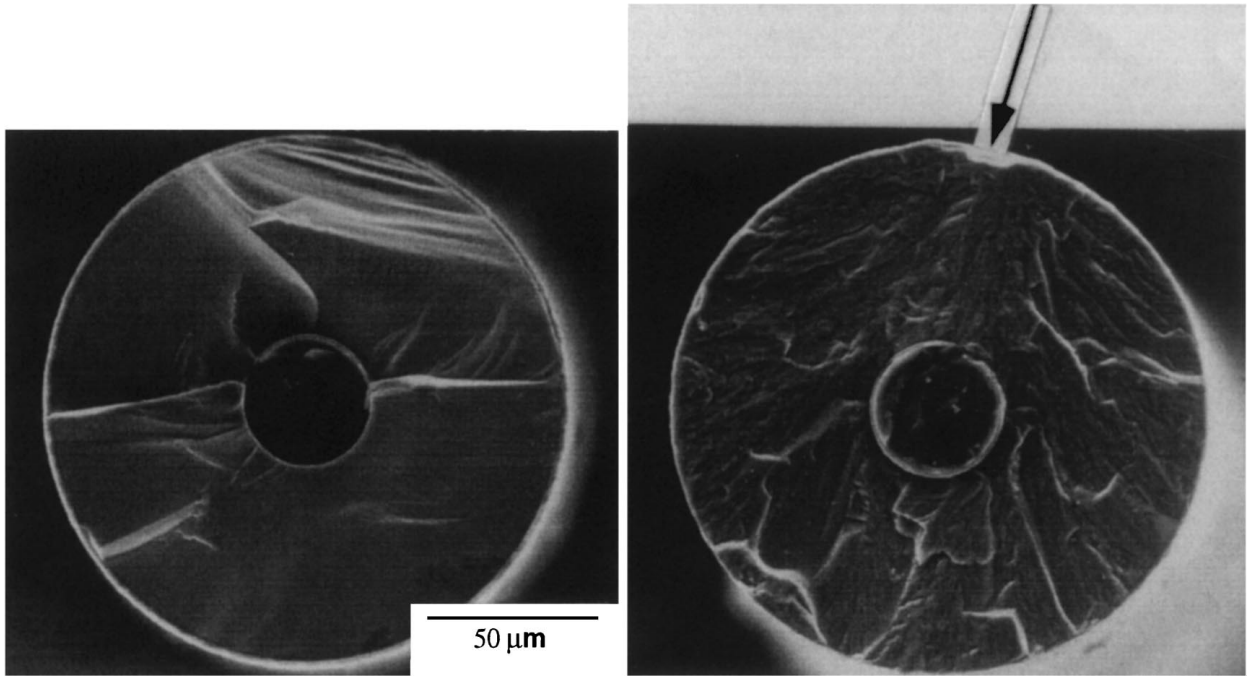

(a) (b)

Figure 20 Secondary SEM image of fracture surface for Ultra SCS fiber depicting: (a) secondary and (b) surface initiations.

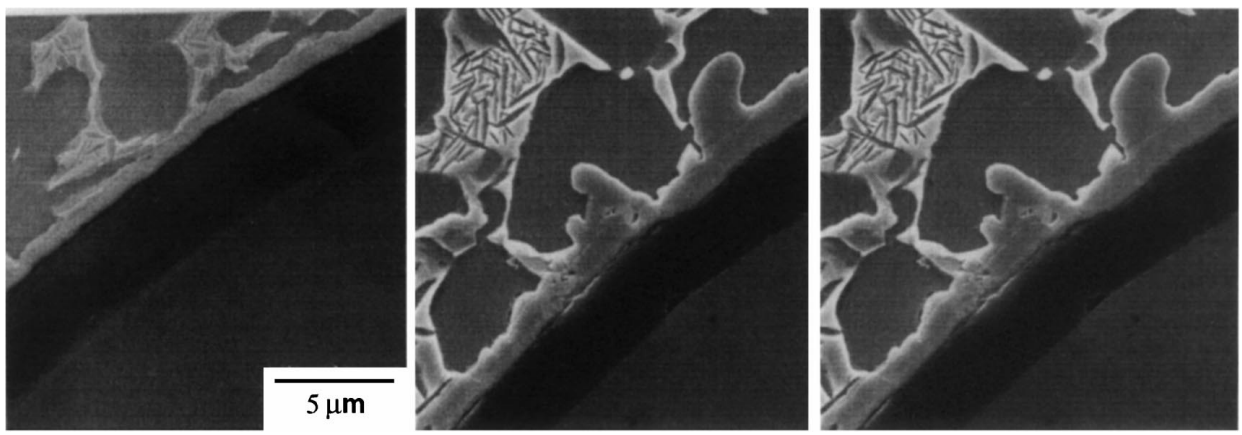

(a) (b) (c)

Figure 21 SCS-6/Ti-22Al-23Nb interface reactions for: (a) as-consolidated, (b) consolidated + 1085 °C solution HT and (c) consolidated + 1160 °C solution HT conditions.

of the coating may have been modified for the Ultra SCS fiber. It was observed that a significant thickness of coating remains ($\sim$2.75 μm) even after the supertranus heat treatment. Therefore, it is not surprising that the fiber is not significantly degraded by chemical reaction with the matrix during thermal treatment. The SiC microstructure appears to be relatively stable (within the limits of detectability) during thermal exposure. There were no failures identified that appeared to initiate within the SiC (i.e. mid-radius).

In conclusion, the Ultra SCS fiber exhibits the highest post-heat treatment strength of all fibers examined in the present study, and as such, is considered the best candidate for use as a reinforcement in an orthorhombic titanium aluminide matrix for metal matrix composite applications wherein processing and/or heat treatment temperatures are comparable to those used in the subject study.

7. Large diameter Ultra SCS

At the time of this study, this 184 μm diameter fiber was in the very preliminary stages of development at Textron Systems Division (formerly, Textron Specialty Materials). Indeed, only a single batch of fiber (totaling $<$500 g) had been made at the time of this study. The primary benefits associated with a larger diameter fiber include the following: (1) an increased foil thickness can be used for the same fiber volume loading with potential of decreasing foil processing costs and hence composite costs; (2) increased inter-fiber spacing can be realized which may enable higher off-axis strengths to be obtained; and (3) since the CMF does not carry significant load, higher volume fractions of the SiC portion of the fiber may result in even higher fiber tensile strength values. A schematic of the large diameter Ultra SCS fiber is shown in Fig. 22. As for the Ultra SCS fiber, this fiber is manufactured using a single stage

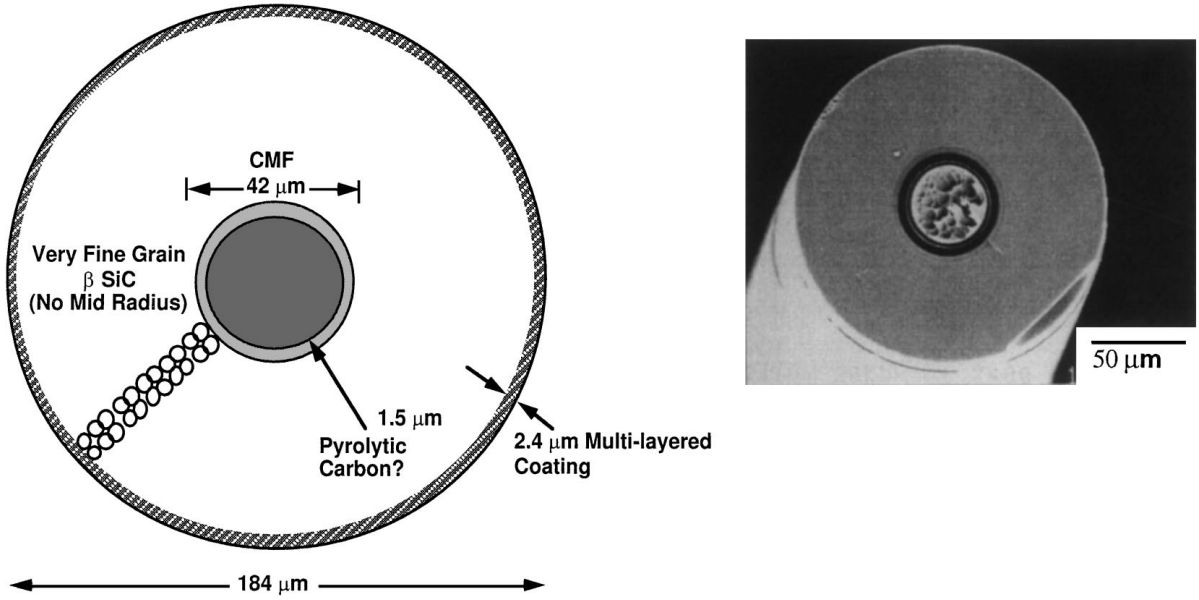

Figure 22 Schematic and secondary SEM image of large diameter Ultra SCS.

CVD reactor. The architecture of the fiber is in many ways analogous to the Ultra SCS fiber. The primary differences between the two fibers include the fiber diameter, a larger diameter CMF (42 μm vs. 33 μm), and a thinner external coating system (2.4 μm vs. 3.3 μm). Note: this coating system has not been optimized and its thickness and chemistry may eventually be modified. Details concerning the chemistry and structure of coating system were not available from Textron at the time of this writing. The most important similarity to Ultra SCS is a very fine β SiC grain size that extends from the CMF to the external coating (with no mid-radius present), and which is thought to provide the very high tensile strengths associated with these fibers.

7.1. Tensile properties, microstructure and fracture analysis

Fig. 23 contains a summary of the heat treatment effect on the tensile strength of large diameter Ultra SCS for all conditions. The mean strength for the as-received condition is 6313 MPa, which was by far the highest strength observed for any of the fibers studied. In fact, 100% of all as-received failures occurred at strength levels >5700 MPa. (Note: once again, these results need to be viewed in the context of this being a single, in fact, first batch of an experimental fiber). This strength value represents an increase of 12.5%, 43% and 103% when compared to the as-received values for Ultra SCS, SCS-6 and Trimarc 1®, respectively. As in

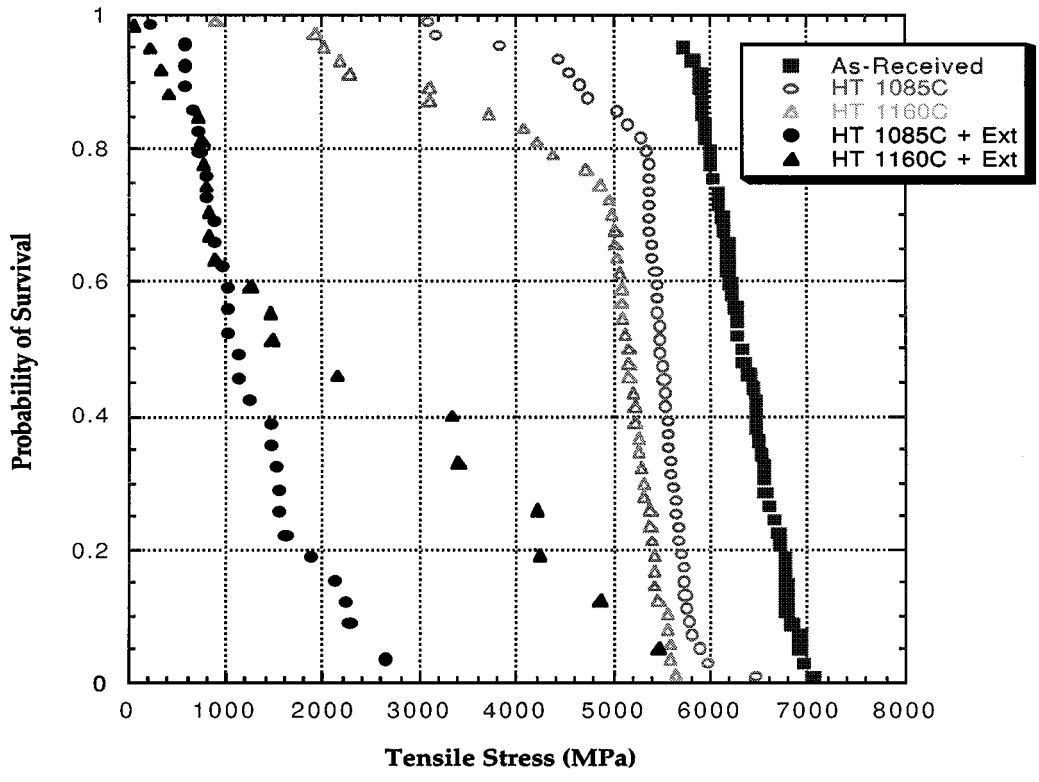

Figure 23 Summary of effect of heat treatment on large diameter Ultra SCS strength.

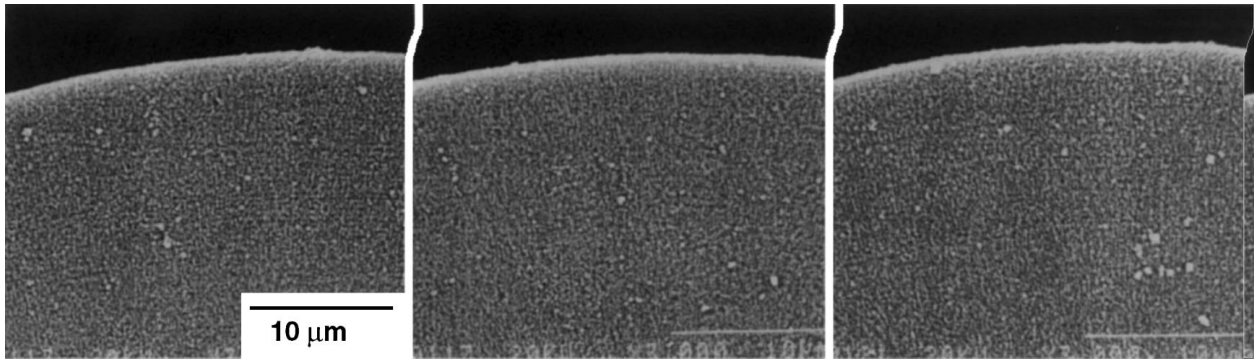

(a) (b) (c)

Figure 24 BSE SEM image of β SiC portion of large diameter Ultra SCS fiber for: (a) as-received, (b) 1085 °C subtransus HT and (c) 1160 °C supertransus HT conditions.

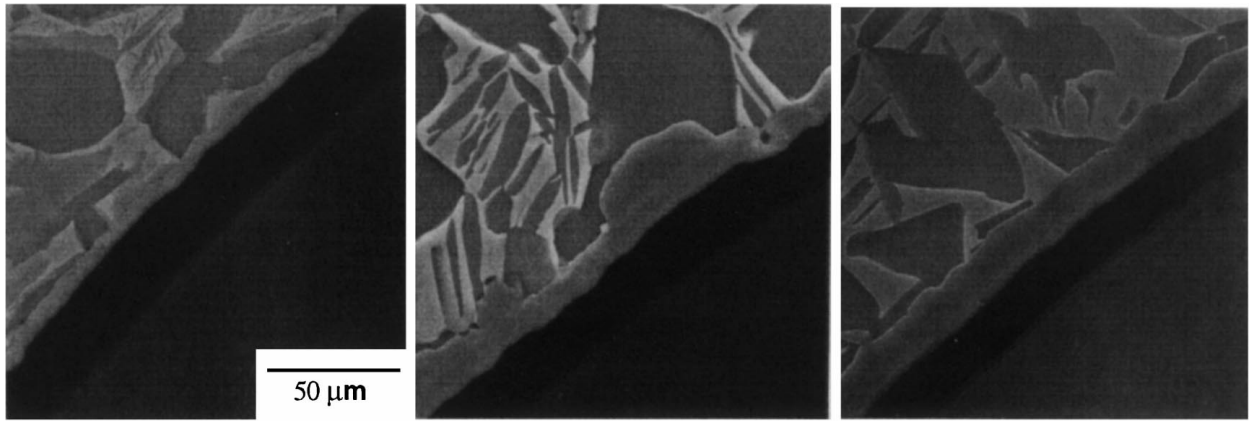

(a) (b) (c)

Figure 25 Large diameter Ultra SCS/Ti-22Al-23Nb reaction zone for: (a) as-consolidated, (b) consolidated + 1085 °C solution HT and (c) consolidated + 1160 °C solution HT conditions.

the case of the Ultra SCS fiber, the source of the high strength is thought to be the fine grain size of the β SiC (Fig. 24a) and perhaps a modification to the external coating system. The increase in strength over the Ultra SCS is thought to be due in part to the higher volume ratio of the β SiC/CMF core. There appears to be a measurable effect of heat treatment on the fiber itself in vacuum. The subtransus heat treated mean strength drops to 5450 MPa (−13%), while the supertransus heat treated strength drops to 5071 MPa (−20%), and for both heat treatments, and there are a fair number of failures (∼20%) at strength levels <5000 MPa. Unfortunately, due to the very high strength and associated energies of fracture, none of the primary fracture surfaces were retained. The β SiC grain structure appears within the detection limits of SEM imaging to be relatively stable with respect to thermal exposure (Fig. 24), and thus, it cannot be conclusively identified as the source of this debit. In addition, since the fiber is deposited upon a CMF, one would not expect reaction between the β SiC and the CMF to have occurred. Therefore, it was not possible to identify the source of weakening at this time.

The effect of both of the heat treatment + extracted conditions is extremely significant. In both conditions a large number of failures (∼80%) occurred at strength levels <2000 MPa. Although as previously noted, the fracture initiation sites could not be identified, one might logically conclude that the reaction with the titanium aluminide matrix may have played a significant role in the degradation observed. Fig. 25 shows the fiber/matrix reaction for this system. The rate of reaction proceeds in a fashion very similar to the Ultra SCS system, but since the initial coating thickness was thinner, the amount of protective coating remaining after exposure is correspondingly less. It is thought that the coating thickness for this experimental fiber may be too thin to provide adequate protection from chemical reaction with the Ti-22Al-23Nb matrix during heat treatment.

In conclusion, the large diameter fiber shows great potential in terms of as-produced strengths, but in its present experimental form, is unsuitable for use as a reinforcement in an orthorhombic titanium aluminide matrix for metal matrix composite applications wherein processing and/or heat treatment temperatures meet or exceed those used in the subject study.

8. Conclusions

Trimarc 1®

- Trimarc 1® exhibited the lowest as-produced tensile strength values for all the fibers evaluated (mean strength = 3080 MPa).
- Significant fiber strength degradation occurred for all heat treatments due primarily to tungsten

core/SiC reaction and possibly fiber/matrix chemical reaction.
- The β SiC microstructure appeared to be thermally unstable upon subtransus and supertransus heat treatment.
- This fiber should not be considered as a candidate reinforcement in orthorhombic titanium aluminide composites (O TMCs).

SCS-6

- The SCS-6 fiber exhibits good as-produced room temperature tensile strength (mean strength = 4303 MPa).
- There was no discernible effect of heat treatment on the tensile strength of the SCS-6 fiber (93% of failures > 3000 MPa).
- Almost all low strength failures were associated with surface flaws, which were likely not a result of fiber/matrix chemical reaction, but instead due to manufacturing/handling.
- There may be a very slight thermal instability of the β SiC structure, however, there was no effect on the fiber tensile strength.
- The SCS-6 fiber should be considered a good candidate for the reinforcement of O TMCs.

Ultra SCS

- The Ultra SCS fiber exhibits excellent as-produced room temperature tensile strength (mean strength = 5610 MPa).
- There was only a very modest effect of heat treatment on the tensile strength of the Ultra SCS fiber (96% of failures > 4000 MPa).
- Almost all low strength failures were associated surface flaws which were likely not a result of fiber/matrix chemical reaction, but due to manufacturing/handling.
- Single stage CVD processing in combination with possibly a slight chemistry modification result in a very fine equiaxed β SiC structure, which is most likely responsible for the very high tensile strength for this fiber.
- The Ultra SCS fiber should be considered as an excellent candidate for the reinforcement of O TMCs.

Large diameter Ultra SCS

- The large diameter (184 μm) Ultra SCS fiber exhibits outstanding as-produced room temperature tensile strength (mean strength = 6313 MPa; 100% of failures > 5700 MPa).
- This fiber exhibits significant reductions in tensile strength when heat treated, particularly within the orthorhombic matrix alloy (0.5 Probability of Survival $\leq$ 1500 MPa).
- The strength debits are suspected to be the result of an unoptimized fiber surface coating, which may be too thin to protect the fiber from chemical reaction with the orthorhombic matrix alloy.
- Although offering tremendous potential in terms of as-produced strength, the large diameter Ultra SCS fiber should not be considered a candidate for the reinforcement of O TMCs in its present form.

Acknowledgements

The authors would like to thank Textron Specialty Materials Division and Atlantic Research Corp. for supplying the continuous SiC fibers and composite materials for this study. Special thanks to Prof. Frank Wawner of the Univ. of Virginia for sample preparation and SEM examination of the SiC fibers for microstructural analysis. Additionally, the authors would like to express their gratitude to Mr. Mark Dodd of Universal Energy Systems who performed the fiber heat treatments.

References

1. P. R. SMITH, J. A. GRAVES and C. G. RHODES, in "Structural Intermetallics," edited by R. Darolia *et al.* (TMS, Warendale, PA, 1993) pp. 765–771.
2. P. R. SMITH, J. A. GRAVES and C. G. RHODES, in "Intermetallic Matrix Composites II," edited by D. B. Miracle, D. L. Anton, and J. A. Graves, Vol. 273 (MRS Sym Proc., Pittsburgh, PA, 1994) pp. 43–52.
3. D. B. MIRACLE, P. R. SMITH and J. A. GRAVES, in "Intermetallics Composites III," edited by J. A. Graves, R. R. Bowman, and J. J. Lewandowski, Vol. 350 (MRS Sym Proc., Pittsburgh, PA, 1994) pp. 133–142.
4. J. A. GRAVES, P. R. SMITH and C. G. RHODES, in "Intermetallic Matrix Composites II," edited by D. B. Miracle, D. L. Anton, and J. A. Graves, Vol. 273 (MRS Sym Proc., Pittsburgh, PA, 1994) pp. 31–42.
5. P. R. SMITH and W. J. PORTER, "The effect of a post-consolidation heat treatment on the tensile and creep behavior of neat matrix Ti-22Al-23Nb," submitted to *J. Mater. Sci.*
6. K. KRISHNAMURTHY and D. B. MIRACLE, "On the role of carbon diffusion during fiber/matrix reaction in SiC fiber reinforced Ti-based MMCs," to be presented at Eleventh International Conference on Composite Materials (ICCM-11), Gold Coast, Queensland, Australia, 14–17 July 1997 (published in proceedings).
7. M. L. GAMBONE and F. E. WAWNER, in "Intermetallics Composites III," edited by J. A. Graves, J. A. Graves, R. R. Bowman and J. J. Lewandowski, Vol. 350 (MRS Sym Proc., Pittsburgh, PA, 1994) pp. 111–118.
8. C. G. RHODES, J. A. GRAVES, P. R. SMITH and M. R. JAMES, in "Structural Intermetallics," edited by R. Darolia *et al.* (TMS, Warendale, PA, 1993) pp. 45–52.
9. I. M. SUKONNIK, P. R. SMITH, J. A. GRAVES, C. G. RHODES, M. C. SHAW, S. KRISHNAMURTHY and A. PANDEY, in Proc. Titanium Matrix Composites Workshop, edited by P. R. Smith and W. C. Revelos, Report No. WL-TR-92–4035, Materials Directorate, Wright Laboratory, WPAFB, OH, April 1992, pp. 98–114.
10. V. FRY, Advanced chemical vapor deposition (CVD) fibers for metal matrix composites, Report No. WL-TR-93–4050, Materials Directorate, Wright Laboratory, WPAFB, OH, April 1993.
11. M. L. GAMBONE, Materials Directorate, WPAFB, OH, unpublished research, 1996.
12. P. R. SMITH, C. G. RHODES and W. C. REVELOS, in Proc. Titanium Aluminide Composite Workshop, edited by P. R. Smith, S. J. Balsone, and T. Nicholas, Report No. WL-Tr-91–4020, Materials Directorate, Wright Laboratory, WPAFB, OH, Feb. 1991, pp. 178–201.
13. C. G. RHODES, in "*Intermetallic Matrix Composites II*," edited by D. B. Miracle, D. L. Anton, and J. A. Graves, Vol. 273 (MRS Sym Proc., Pittsburgh, PA, 1994) pp. 17–31.
14. M. L. GAMBONE and D. B. GUNDEL, in Proc. CMMC'96, San Sebastian, Spain (Sept. 1996).

15. X. J. NING, P. PIROUZ and K. P. D. LAGERLOF, *J. Mater. Res.* **5** (12) (1990) 2865–2876.
16. X. J. NING and P. PIROUZ, *J. Mater. Res.* **6** (10) (1991) 2234–2248.
17. F. E. WAWNER, in "Fibre Reinforcements for Composite Materials," edited by A. R. Bunsell (Elsevier Science Publishers, N. Y., 1988) pp. 371–425.
18. S. R. NUTT and F. E. WAWNER, *J. Mater. Sci.* **20** (1985) 1953.
19. J. D. CASEY and J. GELLER, in Proc. Titanium Aluminide Composite Workshop, edited by P. R. Smith, S. J. Balsone, and T. Nicholas, Report No. WL-Tr-91–4020, Materials Directorate, Wright Laboratory, WPAFB, OH, Feb. 1991, pp. 59–72.
20. M. L. GAMBONE, D. B. GUNDEL and F. E. WAWNER, in Proceedings of 17th Conference on Metal Matrix, Carbon, and Ceramic Matrix Composites, NASA Conf. Pub. # 3225, Part 1, May 1994, 235–252.

Received 9 June 1997
and accepted 14 September 1998